© 2017 IEEE. Personal use of this material is permitted. Permission from IEEE must be obtained for all other uses, in any current or future media, including reprinting/republishing this material for advertising or promotional purposes, creating new collective works, for resale or redistribution to servers or lists, or reuse of any copyrighted component of this work in other works.

Grasping Posture Estimation for a Two-Finger Parallel Gripper with Soft Material Jaws using a Curved Contact Area Friction Model

Jingyi Xu, Nicolas Alt, Zhongyao Zhang and Eckehard Steinbach

***Abstract*— We present a friction model for the curved contact area between a deformable object and soft parallel gripper jaws for grasping posture estimation. We show that the assumption of a planar contact area leads to an overestimation of the frictional force and torque, which might cause the object to slip. We simulate the contact with the Finite Element Method, then compute the friction wrenches, which are fitted with two limit surface models: an ellipsoid and a convex 4th-order polynomial. Despite a slightly higher fitting error, the ellipsoid limit surface is chosen to compute the grasp quality because of its simplicity. We compare the limit surfaces of our friction model with the planar contact model and show the improved accuracy obtainable with our model. We then apply the presented model for grasping posture estimation by simulating the contact for all grasp candidates. We show a grasp quality map (quality of all grasp candidates) and the best possible grasp location for several deformable objects.**

I. INTRODUCTION

The grasp stability is essential for evaluating the grasping posture for an object. Hence, the external disturbances that can be balanced for this posture are often used as quality metrics. These metrics require accurate contact information, such as the maximum frictional force and torque. This information is especially important for grasping easily breakable objects or deformable thin-walled bottles, such as plastic cups. If the applied force becomes too large, the object might be damaged caused by the grasp, or the content of an open bottle might spill due to an excessive deformation. For these objects, gripper fingers with soft pads are widely used to prevent such damage and to increase the stability of grasps due to the larger contact area achievable with deformable jaws. In this paper, we focus on grasp planning for deformable objects which are grasped with a parallel gripper equipped with passive soft foams, such as the visuo-haptic gripper (VH gripper) in [1]–[3]. We simulate the contact using the Finite Element Method (FEM) and study the friction model of a non-planar contact area caused by the soft foam, as shown in Fig. 1. The friction model is then used to determine grasp quality measures.

One major advantage of the visuo-haptic gripper (VH gripper) is that the contact profile can be determined with very low effort and at very low cost. A camera (either mounted on the gripper or placed nearby as shown in Fig. 1) observes the deformation of the foam during the contact. Active contour models [4] are used to track the deformation of the foam contour from the images. Then, the pressure distribution is determined based on a pre-computed deformation model.

Jingyi Xu, Nicolas Alt, Zhongyao Zhang and Eckehard Steinbach are with Chair of Media Technology, Technical University of Munich, Germany Email: {jingyi.xu, n.alt, zhongyao.zhang, eckehard.steinbach}@tum.de

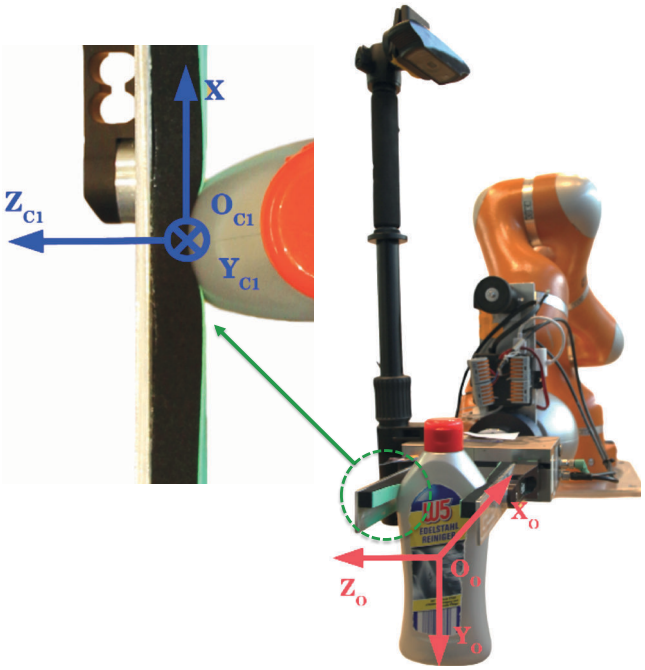

Fig. 1: Curved contact area of the visuo-haptic gripper equipped with soft material jaws.

Another advantage of the VH gripper is the larger contact area compared to rigid gripper jaws, which leads to larger frictional torques. However, the friction model of a non-planar contact has not been well defined, since the friction wrenches and the limit surface (LS) are in $\mathbb{R}^6$ and the exact shape of the LS is difficult to model.

In this paper we propose an extension of the friction model used for the planar contact to compute the friction wrenches $\boldsymbol{w} \in \mathbb{R}^6$ of the curved contact area. For a specific contact, we first use the FEM simulation to determine the deformation of the object and the gripper. The FEM provides the contact pressure and the area of each finite element on the curved contact area. We then compute the $6D$ friction wrenches of each element and the total wrenches $\boldsymbol{w}$ of the curved contact area. This is done by sampling different locations of the center of rotation (COR) of the contact. And for each location, we determine the direction of the frictional force for each element. After that, we approximate $\boldsymbol{w}$ and convert it to a $3D$ wrench $\boldsymbol{w}_{app} \in \mathbb{R}^3$. The wrenches $\boldsymbol{w}_{app}$ are fitted

with an ellipsoid proposed by Howe and Cutkosky [5] and a convex 4th-order polynomial (cvx4thPoly) proposed by Zhou et al. [6]. In our experiments, we choose the ellipsoid as our contact model for its simpler geometrical characteristics and compute the eccentricity parameter e_n of the ellipsoid for the grasp score computation.

To find the optimal grasp location for a query object, we simulate the contact of grasp candidates for the object and store the eccentricity parameter e_n for each contact into a map, referred to as the e_n map. With the e_n map and the known geometry of the object, we compute the grasp quality metric online using the grasping simulator GraspIt! [7].

We present the friction wrenches for our friction model and for the planar contact model with respect to the applied normal force and the curvature of the contact area. We then compare the results by determining the fitting errors of the two LS models. Finally, we illustrate the e_n map and the corresponding grasp quality map for multiple deformable test objects based on the ellipsoidal LS model. The location with the highest score is finally chosen for grasping.

II. Related work

For friction modeling of planar contacts, Goyal et al. [8] proposed the so called limit surface (LS), which captures the relationship between frictional forces, torques and relative motion. For grasp stability analysis, the LS is essential to determine whether a slip will occur for a given external disturbance force and torque pair. Howe and Cutkosky [5] proposed an ellipsoidal approximation of the LS and introduced the facet effects of the LS caused by the discontinuous pressure distribution of a contact. Zhou et al. [6] proposed a convex 4th-oder polynomial force-motion model for planar sliding based on the concept of maximum work inequality [9], which increases the accuracy of the LS fitting.

When grasping deformable objects, the shape of the contact area and the pressure distribution are required to compute the friction and obtain the LS. Ciocarlie et al. [10] use the Finite Element Method (FEM) to simulate the deformation of a soft finger which is in contact with a face of a rigid cube. The maximum frictional force and torque are then computed to construct an ellipsoidal LS. Finally, they compute the grasp wrench space (GWS) by linearizing the ellipsoid and compute the grasp score using the metric proposed by Ferrari and Canny [11].

Following this work, Ciocarlie et al. [12] studied the contact between deformable objects and fingers with curved surfaces. They approximate the local geometry of two contacting bodies to obtain the contact profile based on the elastic contact theory. They assume an elliptical shape contact area and compute the pressure distribution using the Winkler foundation model or Hertzian model [13]. The advantage of this technique is its approximation of the contact profile and the LS which allows us to compute the grasp score in real time. However, this method does not work well for contact with corners or edges as it assumes a planar elliptical contact area. This work is extended by Tsuji et al. [14] for grasp planning for a parallel gripper equipped with a deformable sheet. They approximate the object surface around the contact point with a quadric surface and estimate the shape of the planar contact area. The stress distribution is computed accordingly and used for the LS construction and grasp score computation. Harada et al. [15] use a similar approach and consider the gravity of the query object for the grasp quality metric.

III. Theoretical Background

A. Friction model for planar contact areas

Frictional forces and torques of a planar contact are essential for grasp analysis. Here we briefly review the force-motion model of planar sliding based on the Coulomb friction model. This force-motion model is also applicable for the contact of two objects without relative motion, since the maximum static friction is considered in this paper to be identical to the sliding friction. For details please refer to [5] and [8].

For a two-dimensional planar sliding motion, the contact area can be of arbitrary shape. To compute the friction of this contact, we need to determine the direction of motion at each point on the contact surface. The instantaneous motion of the contact area in the plane can be described as a pure rotation around a point. In this contact, translation can be seen as a rotation around a point, which is infinitely far away. The point is defined as the instantaneous center of rotation (COR). If the COR location is known, it is straightforward to calculate the velocity of each point. Howe and Cutkosky [5] assume a known COR location and formulate the relationship between friction and the instantaneous motion by adding up the frictional contribution of each point on the contact area.

As shown in Fig. 2, let A denote the contact area with a known pressure distribution, where O is the friction-weighted pressure center and is computed by:

$$O_{\{x,y\}} = \frac{\int_A \{x,y\}\mu(x,y)p(x,y)dA}{\int_A \mu(x,y)p(x,y)dA}. \tag{1}$$

Let us consider an infinitesimal element I_{xy} with coordinate $[x\ y]^T$, pressure p_{xy} and area a_{xy}. The vector from O to I_{xy} is the torque arm $\boldsymbol{l}_{xy}$ and $\boldsymbol{d}_{xy}$ is the vector from COR to I_{xy}. The instantaneous velocity of I_{xy} is $\boldsymbol{v}_{xy}$, which is a normal vector perpendicular to $\boldsymbol{d}_{xy}$.

The frictional force $\boldsymbol{f}_{xy}$ and torque $\boldsymbol{\tau}_{xy}$ of the element I_{xy} is computed by:

$$\boldsymbol{f}_{xy} = -\mu p_{xy} a_{xy} \boldsymbol{v}_{xy},\ \boldsymbol{\tau}_{xy} = \boldsymbol{f}_{xy} \times \boldsymbol{l}_{xy}, \tag{2}$$

where μ is the friction coefficient.

The total frictional force and torque are computed by integrating over the contact area A:

$$\boldsymbol{f}_A = \begin{pmatrix} f_{A_x} \\ f_{A_y} \end{pmatrix} = \int_A \boldsymbol{f}_{xy}\ dA,\ \boldsymbol{\tau}_A = \begin{pmatrix} 0 \\ 0 \\ \tau_{A_z} \end{pmatrix} = \int_A \boldsymbol{\tau}_{xy}\ dA. \tag{3}$$

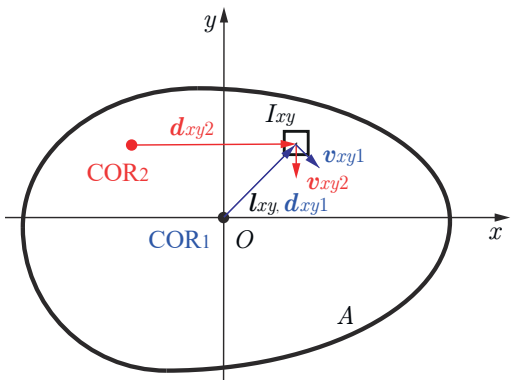

Fig. 2: Examples of the instantaneous velocity $\boldsymbol{v}_{xy}$ of the element I_{xy} depending on the center of rotation (COR) for the planar contact model.

The total torque value $\boldsymbol{\tau}_A$ can be treated as a scalar here, because the torque arm $\boldsymbol{l}$ and the frictional force $\boldsymbol{f}$ are coplanar.

Different COR positions affect the direction of the instantaneous velocity of each small element and thus the friction. As shown in Fig. 2, there are two example COR locations COR_1 and COR_2, where COR_1 coincides with the origin O. The velocity $\boldsymbol{v}_{xy1}$ and $\boldsymbol{v}_{xy2}$ of the element I_{xy} are depend on COR_1 and COR_2, respectively. The total torque value $\boldsymbol{\tau}_A$ is maximum for COR_1, since the torque arm $\boldsymbol{l}$ of each element is perpendicular to the velocity and the frictional force. When the COR is infinitely far away along the x-axis, the velocity of each element is along the y-axis, thus f_{A_y} is maximized.

Howe and Cutkosky [5] showed that $(f_{A_x}, f_{A_y}, \tau_{A_z})$ can be approximated as an ellipsoid. This ellipsoid is called the limit surface (LS) for this contact. The LS can be used to determine the stability of the contact. If the external disturbance force and torque pair lies within the LS, then a slip will not occur, since the friction of the contact is able to resist this disturbance.

B. Grasp analysis

The above mentioned friction model can be used to examine the stability and quality of a grasp. The idea is to determine the external disturbances that this grasp can resist. Here we will briefly describe the method to obtain the classical quality metric of a grasp proposed by Ferarri and Canny [11].

To describe a contact, the contact force $\boldsymbol{f}$ and torque $\boldsymbol{\tau}$ are usually combined into one variable called wrench $\boldsymbol{w} = [\boldsymbol{f}\ \boldsymbol{\tau}]^T$. For a 3D problem, $\boldsymbol{w} \in \mathbb{R}^6$. For a contact i, the process is to first determine the limit surface. Its linear approximation is usually used in practice to simplify the problem. For an ellipsoidal limit surface, its approximation can be obtained by taking the convex hull of m vertices on its surface [12]. The corresponding friction wrenches $\boldsymbol{w}_{i1}, \ \ldots \ \boldsymbol{w}_{im}$ can be computed and transformed into a single frame of reference. This reference frame is usually chosen to be the center of mass of the object, as shown in Fig. 1. The total grasp wrench space (GWS) of n contacts is computed by taking the convex hull of the Minkowski sum of transformed wrenches:

$$W_{L\infty} = ConvexHull(\oplus_{i=1}^{n}\{\boldsymbol{w}_{i1}, \ \ldots \ \boldsymbol{w}_{im}\}). \quad (4)$$

$W_{L\infty}$ is the space of the wrenches that can be applied by the grasp. Thus, it indicates the external disturbances that can be resisted with this grasp. To allow the comparison between different grasps, the magnitude of the normal force of each contact is limited to 1 for grasp score computation [11]. We use the volume of $W_{L\infty}$ as the quality metric of a grasp.

IV. Friction Model for Curved Contact Area

When an object is grasped with soft parallel gripper jaws, the contact area is typically non-planar. The friction wrenches are in $\mathbb{R}^6$. Thus, the ellipsoidal limit surface model proposed by Howe and Cutkosky [5] is not directly applicable. In the following, we propose a friction model for the curved contact area in $\mathbb{R}^6$ and compute its approximation in $\mathbb{R}^3$, such that the existing limit surface models can be used for stability analysis and grasp planning.

A. Friction wrench computation

To compute the static friction for a non-planar contact between two bodies, we describe the three-dimensional instantaneous motion of a body as a rotation around a single axis, instead of a point. This rotation axis is the center of rotation (COR) in $3D$ space.

To simplify the problem, we convert the grasp wrench space (GWS) $\boldsymbol{w} \in \mathbb{R}^6$ of contact i into an approximated wrench $\boldsymbol{w}_{app} \in \mathbb{R}^3$ for the limit surface construction. We choose $\boldsymbol{w}_{app} = [f_{xi}, f_{yi}, \tau_{zi}]^T$, because $f_{xi}, f_{yi} \gg f_{zi}$ and $\tau_{zi} \gg \tau_{xi}, \tau_{yi}$ in general. The coordinates are shown in Fig. 1. We analyze the locations of the COR axis, which is parallel to the z_i axis for contact i, such that the maximum of $(f_{xi}, f_{yi}, \tau_{zi})$ can be determined. This is done because we want to compute the maximum friction of the contact to analyze the grasp stability. If the COR axis is not parallel to the z_i axis in Fig. 1, then at least one component may not reach its maximum, since it will be partially shifted to the remaining axes. The wrench $\boldsymbol{w}_{app}$ is then approximated by setting the remaining components in $\boldsymbol{w}$ to 0.

Similar to the LS model for planar contact, we divide the curved contact area into small elements and compute the friction for each element by assuming a known COR location and a pressure distribution, as shown in Fig. 3(a). In this work, we use the Finite Element Method (FEM) to simulate the contact between the visuo-haptic gripper and a deformable object, such as a plastic bottle. As a result from the FEM simulation, we obtain the contact area and pressure distribution, which allow us to compute the LS of the contact. In real applications, the pressure distribution can be obtained by the deformation of the foam mounted on the gripper or another tactile sensor.

The FEM divides the curved contact area into rectangular finite elements. Each element is assumed to be planar. This

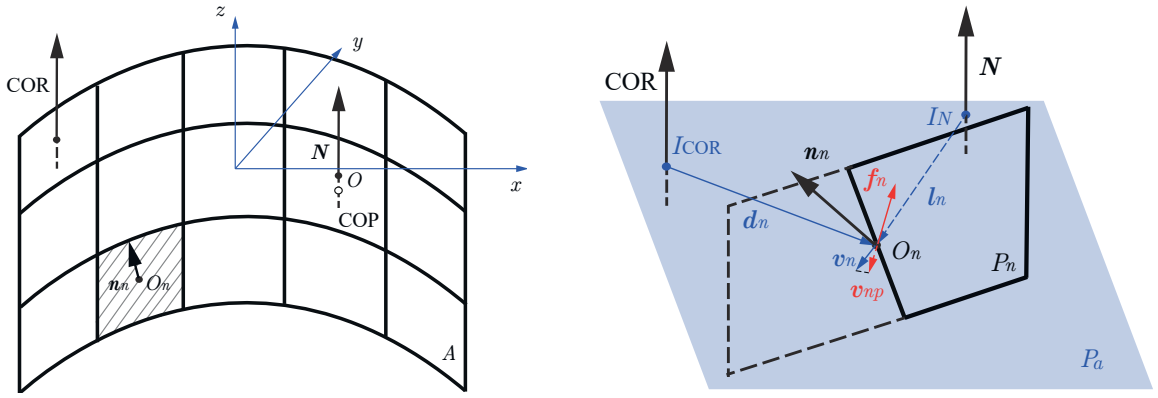

Fig. 3: Example of a curved contact area with origin O and contact normal N. (a): A curved contact area that is devided into small elements. The shadowed rectangle is element n with origin O_n and normal $\boldsymbol{n}_n$. (b): An enlarged view of element n with the projected velocity $\boldsymbol{v}_{np}$ and the frictional force $\boldsymbol{f}_n$.

method is also applicable for triangular elements. The contact normal $\boldsymbol{N}$ is defined by the average normal of all elements that contain the origin. The local contact coordinate system (x, y, z) is defined such that $z \| \boldsymbol{N}$, while x is on the plane perpendicular to z and possibly parallel to the long side of the foam.

To locate the origin O, we first compute the friction-weighted center of pressure (COP) with:

$$COP_{\{x,y,z\}} = \frac{\int_A \{x, y, z\} \mu(x, y, z) p(x, y, z) dA}{\int_A \mu(x, y, z) p(x, y, z) dA}, \quad (5)$$

which is an extension of Eq. 1 in $3D$, where $\mu(x, y, z)$ is the friction coefficient and is assumed to be uniform for this contact.

The COP might not be on the contact surface because of the curvature. Thus, the origin O is the projection of the COP onto the contact area A along the contact normal $\boldsymbol{N}$, as shown in Fig. 3(a).

Fig. 3(b) shows the element n extracted from the contact area A with origin O_n, normal $\boldsymbol{n}_n$ and pressure p_n. The figure also shows an example COR axis, which is parallel to the contact normal $\boldsymbol{N}$.

In order to determine the direction of the frictional force of element n, we need to first determine its velocity $\boldsymbol{v}_n$. The problem of the curved contact area is that the velocity $\boldsymbol{v}_n$ may not be coplanar with the element plane. Since the frictional force is restricted to be on the element plane, so it may not be parallel to the velocity $\boldsymbol{v}_n$. Thus, we compute the projection of the velocity $\boldsymbol{v}_n$ onto the plane, which is denoted as $\boldsymbol{v}_{np}$ and set the frictional force to be parallel to the projected velocity $\boldsymbol{v}_{np}$. This is due to the fact that only the velocity, which is parallel to the plane, affects the frictional force.

To better explain the algorithm, lets create an auxiliary plane denoted as P_a, as shown in Fig. 3(b). Plane P_a is normal to the COR axis and the contact normal $\boldsymbol{N}$, and passes through the element center O_n. Denote the intersection point of the plane P_a and the COR axis as I_{COR}, I_N as the intersection point of P_a and the contact normal $\boldsymbol{N}$. To calculate the velocity $\boldsymbol{v}_n$ for the element n, we first determine the vector $\boldsymbol{d}_n$, which is from I_{COR} to O_n. The velocity $\boldsymbol{v}_n$ is determined by finding a vector, which also lies in the plane P_a and is perpendicular to $\boldsymbol{d}_n$. Please note that in this case, $\boldsymbol{v}_n$ does not lie in the element plane P_n. Thus, we calculate the projected velocity $\boldsymbol{v}_{np}$ of $\boldsymbol{v}_n$ onto the element plane P_n. It is computed by subtracting the component of $\boldsymbol{v}_n$ that is orthogonal to P_n from $\boldsymbol{v}_n$:

$$\boldsymbol{v}_{np} = \boldsymbol{v}_n - \frac{\boldsymbol{v}_n \cdot \boldsymbol{n}_n}{\|\boldsymbol{n}_n\|^2} \boldsymbol{n}_n, \quad (6)$$

where $\boldsymbol{n}_n$ is the normal of the element plane P_n. The direction of the frictional force $\boldsymbol{f}_n$ is opposite of $\boldsymbol{v}_{np}$. After that, the torque arm $\boldsymbol{l}_n$ is determined by the vector from I_N to the element center O_n. Finally, the friction wrench $\boldsymbol{w}_n = [\boldsymbol{f}_n, \boldsymbol{\tau}_n]^T$ is computed by:

$$\boldsymbol{f}_n = [f_{nx}, f_{ny}, f_{nz}]^T = -\mu p_n a_n \frac{\boldsymbol{v}_{np}}{\|\boldsymbol{v}_{np}\|}, \quad (7)$$

$$\boldsymbol{\tau}_n = [\tau_{nx}, \tau_{ny}, \tau_{nz}]^T = \boldsymbol{f}_n \times \boldsymbol{l}_n, \quad (8)$$

where p_n and a_n are the pressure and the area of element n, respectively.

The total friction wrench $\boldsymbol{w}$ of A is computed by summing up the wrench of each element. Similar to the planar contact, when the COR coincides with O, τ_z reaches its maximum, since the frictional forces and torque arms are "more perpendicular" than in other cases. Also, when the COR is located far away along the x axis, f_y becomes maximal.

Please note that in this work, the change of the contact area and the normal pressure caused by the friction wrench is neglected. This is under the assumption that the influence of the tangential friction upon the normal pressure is small, especially when the friction coefficient is less than one [13]. Thus, the normal pressure and the tangential friction can be treated separately.

B. Limit surface fitting

To describe the relationship between the friction and the object motion, the limit surface (LS) is widely used. To find the suitable LS model of the contact, we compute the friction wrenches with different locations of the center of rotation (COR) axis . To obtain the locations, we approximate the curved contact area to a planar rectangle P_r with length $a \times b$ with $a \geq b$. The positions of the COR are obtained by evenly sampling a square P_s with length $10a \times 10a$, where its center is located at the origin of the contact O.

Then, the approximated wrenches $\boldsymbol{w}_{app} = [f_x, f_y, \tau_z]^T$ are fitted with an ellipsoid or a convex 4th-order polynomial (cvx4thPoly) [6]. To ensure all 3 components of the friction wrench have the same unit, Erdmann [16] proposed to normalize the frictional torque τ_z by dividing it with the radius of gyration ρ. Zhou et al. [6] have found that different values of ρ, such as average edge length or radius of the minimum enclosing circle lead to similar performance for the LS construction. Thus, we choose $\rho = a$ for simplicity.

The analysis of the LS fitting error is shown in Sec. VI. Generally, the error of cvx4thPoly is smaller than that for the ellipsoidal model. However, the ellipsoid is chosen for our LS model, because of the simpler geometric characteristics: we only need to compute the friction wrenches corresponding to 3 COR locations, which maximize f_x, f_y and τ_z, respectively, to construct the ellipsoid. In addition, an ellipsoidal LS can be easily described with a single variable referred to as the eccentricity parameter e_n [12], which will be explained in the following section.

V. The Eccentricity Parameter Map and Grasp Location Estimation

When the limit surface (LS) of a contact is modeled with an ellipsoid, the eccentricity parameter e_n can be used to describe the relationship between the maximum frictional force and torque, thus e_n is essential for grasp analysis. Following [5] and [10], the frictional constrains based on the ellipsoidal LS model parameterized with (f_x, f_y, τ_z) can be formulated as :

$$\frac{f_x^2}{\max^2(f_x)} + \frac{f_y^2}{\max^2(f_y)} + \frac{\tau_z^2}{\max^2(\tau_z)} \leq 1. \tag{9}$$

For a planar contact with normal force F_N and friction coefficient μ, denote f_t as the tangential frictional force, where $f_t^2 = f_x^2 + f_y^2$. The maximum frictional force is:

$$\max(f_t) = \max(f_x) = \max(f_y) = \mu F_N. \tag{10}$$

To better describe the ellipsoidal LS, Howe and Cutkosky [5] defined the eccentricity parameter e_n as:

$$e_n = \frac{\max(\tau_z)}{\max(f_t)}. \tag{11}$$

The frictional constraints for a planar contact in Eq. 9 can be formulated as:

$$f_x^2 + f_y^2 + \frac{\tau_z^2}{e_n^2} \leq \mu^2 F_N^2, \text{ where } e_n = \frac{\max(\tau_z)}{\mu F_N}. \tag{12}$$

Thus, with the pre-computed e_n, the ellipsoidal LS can be reconstructed with the semi-principal axes $\mu F_N \cdot [1\ 1\ e_n]^T$ for different F_N values.

However, for a curved contact area, $\max(f_x)$ and $\max(f_y)$ might not be equal to μF_N because of the curvature. For a precise LS reconstruction for a curved contact area, the ellipsoidal LS is parametrized with $[\max(f_x)\ \max(f_y)\ \mu F_N e_n]^T$, where f_x, f_y, e_n all depend on F_N, since the curvature of the contact area varies under different magnitude of normal forces. Thus, the values f_x, f_y, e_n for each normal force need to be pre-computed and stored for the LS reconstruction.

If the required accuracy of the LS is not high, the LS can be reconstructed with the parameters $\mu F_N \cdot [1\ 1\ e_n]^T$ to simplify the process. In this case, the frictional torque is computed with the curved contact area model, while the frictional forces are computed with the planar contact model, which might lead to overestimation of the frictional forces.

In addition, e_n can be used for grasp score computation. We simulate the contact between the two-finger visuo-haptic sensor foam [1], [2] and all grasp candidates of a query object with the same normal force, then compute and store the e_n of each candidate to a map. We refer to this map as the eccentricity parameter (e_n) map. The maximum frictional forces are also stored additionally to increase the grasp score accuracy in this work. With the known geometry and the e_n map of an object, the grasp score can be computed online with the ellipsoidal LS linearization technique [12] and the L_∞ quality metric [11], without knowing the exact contact area and pressure distribution.

The grasp quality for all candidates of the query object are computed and stored to a map, which we refer to as the grasp quality map. The locations with the highest grasping score are considered as the best possible choices for grasping.

VI. Results and Experiments

In order to check the wrench difference between a curved contact model and a planar contact model, we first simulate the contact between the visuo-haptic gripper (VH gripper) in Fig. 1 and multiple rigid elliptic cylinders with a fixed semi axis a and a variable semi axis b with $0.4a \leq b \leq 2.5a$. The contact normal is parallel to a. The magnitude and the direction of the normal force is the same for each simulation in this experiment. Fig. 4(a) shows the simulation results obtained with the FEM software ANSYS® [17]. To simplify the model of the VH gripper, only the two-finger jaws are modeled for the simulation. Each finger consists of the foam and a metal sheet to prevent undesired deformations of the foam. The foam is meshed with hyper-elastic hexahedral elements of type Hyper86 in ANSYS®. The metal sheet and the elliptical cylinder are meshed with tetrahedral elements of type solid187. As shown in Fig. 4(a), the pressure is evenly applied on the metal sheets of both fingers, such that the normal forces are parallel to the contact normal. The contact profile is extracted from the finite elements of the VH gripper, as shown in Fig. 4(b). The green line is the contact normal. For each element, the color dot is the

simulated pressure value, the arrow shows the direction of the computed frictional force based on the curved contact model, when the COR-axis coincides with the origin O, indicated with a blue dot. Fig. 4(c) shows the difference of frictional force and torque between the curved and the simplified planar contact model, where the x-axis is the curvature of the contact area. Since the elliptic cylinder is rigid, the curvature of the contact area is controlled by the ratio of the two semi axis of the ellipse a and b. Thus, the curvature equals a/b. This figure shows that the difference grows with the curvature of the contact area.

Next, we simulate multiple contacts between the VH gripper and a thin-walled deformable test object for grasp planning. The geometry of the real object is shown in Fig. 8(a). The 3D model for the FEM simulation is built manually, for details please refer to [18]. As shown in Fig. 5(a), there are 70 grasp candidates for the test object. Each contact of the object and the VH gripper is simulated, where the center of the VH gripper is located at one grasp candidate and the contact normal is parallel to the vector from the location of the grasp candidate to the center axis of the object. The test object is meshed with thin-shell elements of type SHELL181 in ANSYS®. Fig. 5(a) shows the asymmetric contact area extracted from the VH gripper located on the grasp candidate x31 near the neck of the test object, where the normal force is 3N and the COR-axis coincides with the origin. Fig. 5(b) shows the space of the friction wrenches for this contact. The wrenches are obtained by densely sampling the locations of the COR-axis with the proposed curved contact model (CCM) and the existing planar contact model (PCM). The frictional torque is normalized by dividing it by the length of the contact area such that all 3 components of each approximated wrench $\boldsymbol{w}_{app}$ have the same unit. For details please refer to Sec. IV-B.

As expected, the wrenches of the PCM are larger than the CCM, since the PCM model does not consider the fact that the frictional force of each element has to be restricted on the plane of the element and thus leads to an overestimation of the friction. Please note that the facets on the surface of the LS are caused by the discontinuous pressure distribution from the FEM simulation. For a real contact between the gripper and the object, the pressure distribution is continuous. Thus, the facets are neglected by the LS fitting.

Fig. 6(a) and (b) show the fitted LS with the convex 4th-order polynomial (cvx4thPoly) and the ellipsoidal model of this contact with fewer wrench data, indicated with red dots. The code for the LS fitting is provided by Zhou [6]. It is easy to see that many wrench data points are inside the ellipsoidal LS, while the most data points are on the surface of the cvx4thPoly LS. Hence, the ellipsoidal LS has a larger fitting error than the cvx4thPoly. Fig. 6(c) shows the fitting error of both LS models with the curved contact model for all 35 grasp locations along the x-axis of the test object.

For the same contact location x31, Fig. 7(a) shows the normalized maximal frictional force of the curved contact model (CCM) and the simplified planar contact model (PCM) with an increasing normal force. We chose the friction

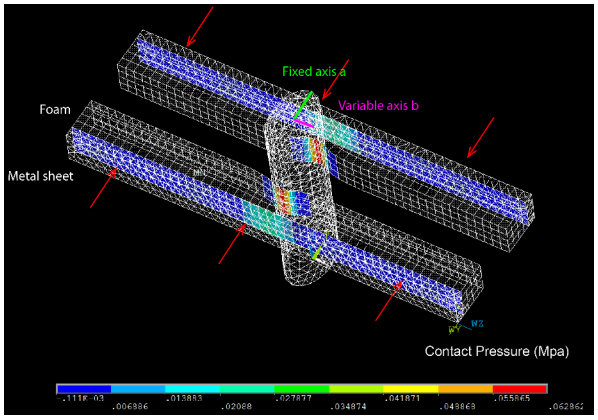

(a) FEM simulation of the contact between an elliptical cylinder and the visuo-haptic two-finger gripper.

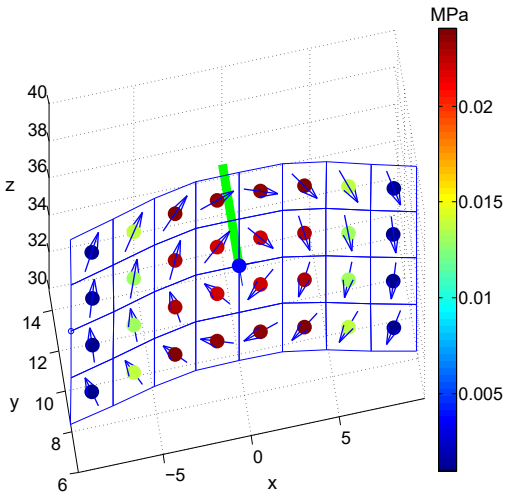

(b) Extracted curved contact area with its pressure distribution and the computed frictional forces.

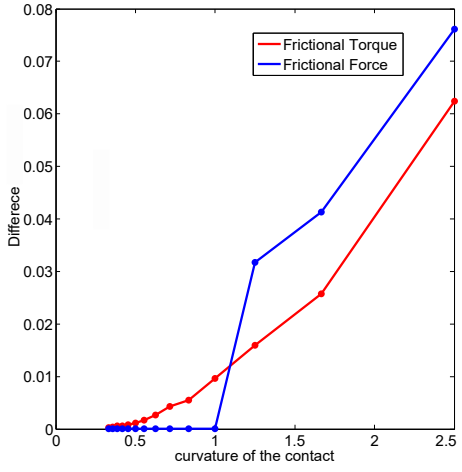

(c) The difference of the frictional force and torque between the curved and the planar contact model as a function of the contact curvature.

Fig. 4: Contact simulation between elliptical cylinders with variable axis length and the two-finger gripper.

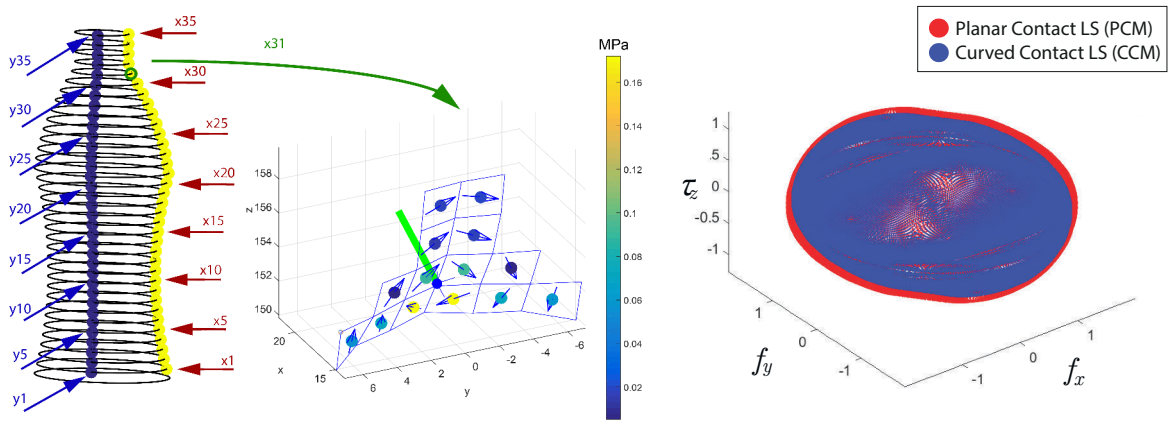

(a) (b)

Fig. 5: (a): 70 grasp candidates of the test object and the contact information of the grasp candidate x31. (b): Comparison of friction wrenches with densely sampled CORs.

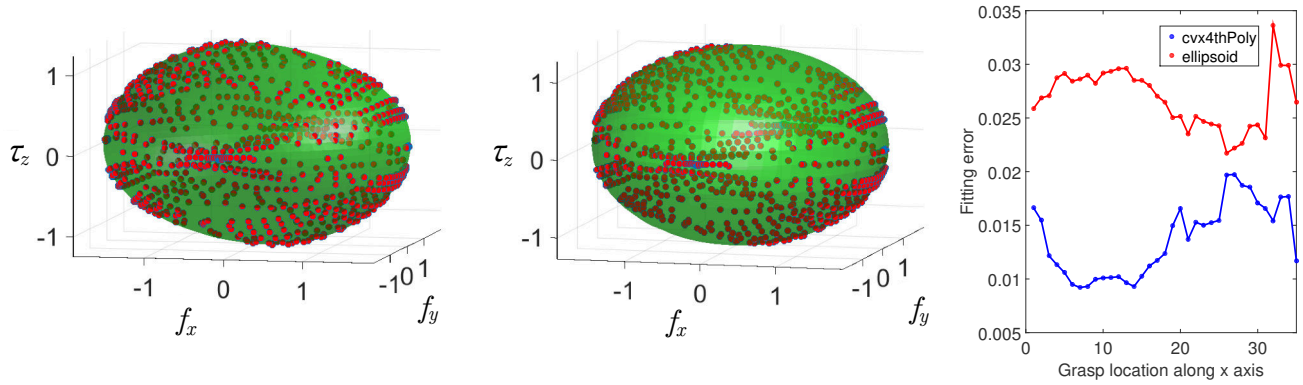

(a) Fitted LS with the convex 4th-order polynomial model. (b) Fitted LS with the ellipsoidal model. (c) Fitting error comparison.

Fig. 6: Fitted limit surfaces for grasp candidate x31 and the fitting error comparison for 35 grasp locations.

coefficient $\mu = 2$. The normalized frictional force and torque are computed by scaling the normal force to 1 for the grasp score computation. Hence, the frictional force of the PCM is constant and the force of the CCM varies depending on the curvature and the shape of the contact area. Fig. 7(b) shows the normalized maximal frictional torque, which is normalized by dividing it by the length of the maximum contact area of all contacts. The torque is normalized this way, such that it has same unit as the force for grasp score computation. The second reason is that the frictional torque caused by different normal forces becomes comparable. It grows with enlarged magnitude of the normal force because of the increased contact area.

Fig. 7 (c) and (d) show the eccentricity parameter e_n and the normalized grasp score, respectively. The score is computed based on frictional forces, e_n and the ellipsoidal LS model, as described in Sec.V.

Fig. 8 shows the eccentricity parameter e_n map and the grasp quality map for two test objects. For the e_n maps, the largest e_n values are not at the widest part of the object. This is because in both cases, the contact area at the widest part has a bump, such that the pressure is smaller than for other locations. For grasp score computation, the object length along the x, y, z direction is scaled to 1, such that the total torque caused by the contact does not depend on the object's size. The locations with highest grasp score are chosen as the best possible grasping locations.

VII. Conclusion and Outlook

We presented a friction model for non-planar contacts between an object and a two-finger gripper, which is equipped with soft material jaws. A Finite Element Method based simulation is used to obtain the contact profile. We then computed and fitted the friction wrenches with the ellipsoidal and the convex 4th-order polynomial (cvx4thPoly) model. The former is chosen and its eccentricity parameter of the contact with each grasp candidate for the query object is pre-computed and stored in the eccentricity parameter map for grasp score computation. The optimal grasping posture of the object is obtained by selecting the highest score.

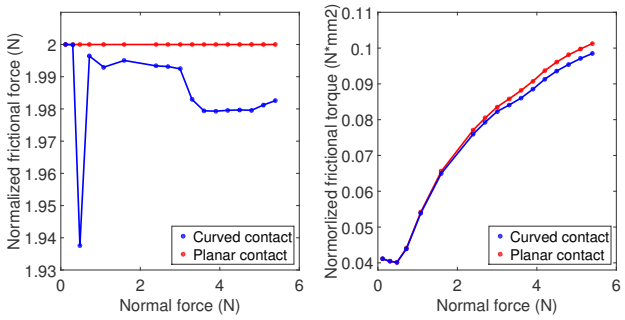

(a) Normalized frictional force. (b) Normalized frictional torque.

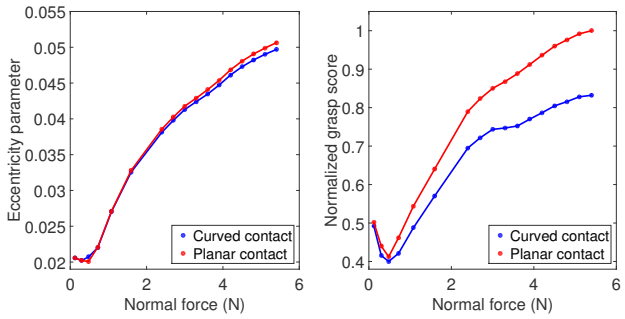

(c) Eccentricity parameter e_n. (d) Normalized grascp score.

Fig. 7: Frictions, e_n and grasp scores of the curved contact and the simplified planar contact model with increased normal force for the grasp candidate x31.

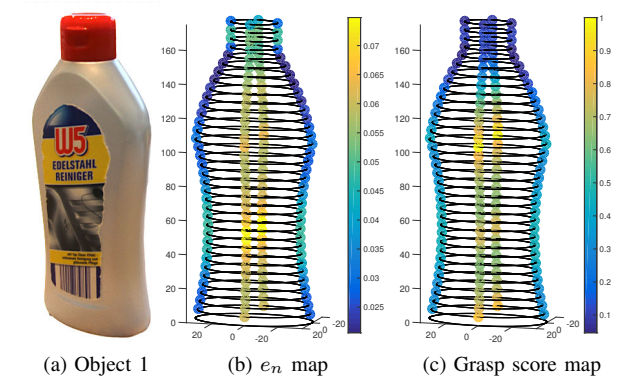

(a) Object 1 (b) e_n map (c) Grasp score map

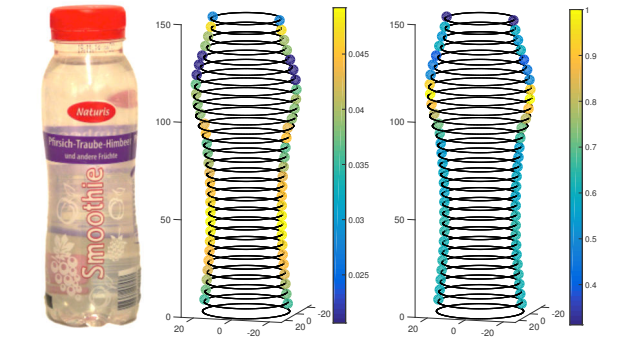

(d) Object 2 (e) e_n map (f) Grasp score map

Fig. 8: Eccentricity parameter map and grasp score map of two test objects.

In future work, we will use the convex 4th-order polynomial as the limit surface (LS) model and use it for the evaluation of the grasp quality. We will explore the eccentricity parameter of this model and the relationship of the LS depending on the object shape and material properties, such as Young's modulus and passions ratio, such that the LS of each contact can be computed without simulation. Furthermore, we will combine other quality metrics of grasp planning for deformable objects, such as considering the stiffness of the objects at the grasp locations and possible disturbance wrenches such as the gravity.

REFERENCES

[1] N. Alt and E. Steinbach, "Navigation and manipulation planning using a visuo-haptic sensor on a mobile platform," *IEEE Transactions on Instrumentation and Measurement*, vol. 63, no. 11, 2014.

[2] N. Alt, J. Xu, and E. Steinbach, "Grasp planning for thin-walled deformable objects," in *Robotic Hands, Grasping, and Manipulation (ICRA Workshop)*, Seattle, WA, USA, May 2015.

[3] N. Alt and E. Steinbach, "A visuo-haptic sensor for the exploration of deformable objects," in *Int. Workshop on Autonomous Grasping and Manipulation: An Open Challenge, in conjunction with IEEE International Conference on Robotics and Automation (ICRA 2014)*, Hong Kong, May 2014.

[4] M. Kass, A. Witkin, and D. Terzopoulos, "Snakes: Active contour models," *International journal of computer vision*, vol. 1, no. 4, pp. 321–331, 1988.

[5] R. D. Howe and M. R. Cutkosky, "Practical force-motion models for sliding manipulation," *The International Journal of Robotics Research*, vol. 15, no. 6, pp. 557–572, 1996.

[6] J. Zhou, R. Paolini, J. A. Bagnell, and M. T. Mason, "A convex polynomial force-motion model for planar sliding: identification and application," in *2015 IEEE International Conference on Robotics and Automation (ICRA)*. IEEE, 2016, pp. 2319–2325.

[7] A. T. Miller and P. K. Allen, "Graspit! a versatile simulator for robotic grasping," *IEEE Robotics & Automation Magazine*, vol. 11, no. 4, pp. 110–122, 2004.

[8] S. Goyal, A. Ruina, and J. Papadopoulos, "Planar sliding with dry friction part 1. limit surface and moment function," *Wear*, vol. 143, no. 2, pp. 307–330, 1991.

[9] J. J. Moreau, "Unilateral contact and dry friction in finite freedom dynamics," in *Nonsmooth mechanics and Applications*. Springer, 1988, pp. 1–82.

[10] M. Ciocarlie, A. Miller, and P. Allen, "Grasp analysis using deformable fingers," in *2005 IEEE/RSJ International Conference on Intelligent Robots and Systems*. IEEE, 2005, pp. 4122–4128.

[11] C. Ferrari and J. Canny, "Planning optimal grasps," in *Robotics and Automation, 1992. Proceedings., 1992 IEEE International Conference on*. IEEE, 1992, pp. 2290–2295.

[12] M. Ciocarlie, C. Lackner, and P. Allen, "Soft finger model with adaptive contact geometry for grasping and manipulation tasks," in *Second Joint EuroHaptics Conference and Symposium on Haptic Interfaces for Virtual Environment and Teleoperator Systems (WHC'07)*. IEEE, 2007, pp. 219–224.

[13] K. L. Johnson and K. L. Johnson, *Contact mechanics*. Cambridge university press, 1987.

[14] T. Tsuji, S. Uto, K. Harada, R. Kurazume, T. Hasegawa, and K. Morooka, "Grasp planning for constricted parts of objects approximated with quadric surfaces," in *2014 IEEE/RSJ International Conference on Intelligent Robots and Systems*. IEEE, 2014, pp. 2447–2453.

[15] K. Harada, T. Tsuji, S. Uto, N. Yamanobe, K. Nagata, and K. Kitagaki, "Stability of soft-finger grasp under gravity," in *2014 IEEE International Conference on Robotics and Automation (ICRA)*. IEEE, 2014, pp. 883–888.

[16] M. Erdmann, "On a representation of friction in configuration space," *The International Journal of Robotics Research*, vol. 13, no. 3, pp. 240–271, 1994.

[17] ANSYS® Academic Research, Release 16.2.

[18] N. Alt, J. Xu, and E. Steinbach, "A dataset of thin-walled deformable objects for manipulation planning," in *Grasping and Manipulation Datasets (ICRA Workshop)*, Stockholm, Sweden, May 2016.